

# Regulation of Cell Growth and Expression of 7B2, PC2, and PC1/3 by TGF $\beta$ 1 and Sodium Butyrate in a Human Pituitary Cell Line (HP75)

Ikuo Kobayashi,<sup>1,2</sup> Long Jin,<sup>1</sup> Katharina H. Ruebel,<sup>1</sup>  
Jill M. Bayliss,<sup>1</sup> Oka Hidehiro,<sup>2</sup> and Ricardo V. Lloyd<sup>1</sup>

<sup>1</sup>Department of Laboratory Medicine and Pathology, Mayo Clinic and Mayo Foundation, Rochester,

<sup>2</sup>Minnesota and Department of Neurosurgery, Kitasato University School of Medicine, Sagamihara, Kanagawa, Japan

Recent studies have shown that 7B2 and the neuroendocrine-specific proconvertase PC2 have important roles in pituitary cell proliferation and hormone secretion. Studies from our laboratory have also shown that TGF $\beta$ 1 regulates anterior pituitary cell proliferation and hormone secretion.

To study the regulation of 7B2 in human pituitary tumors, we used a cell line derived from a human pituitary adenoma (HP75) that has been shown to express 7B2, PC1, PC2, and TGF $\beta$  receptors to analyze the effects of TGF $\beta$ 1 and the histone deacetylase inhibitor (HDACI) sodium butyrate (NaB) treatment on 7B2 mRNA expression along with the neuroendocrine-specific proconvertases 1/3 (PC1) and PC2 mRNA and protein expression. RNA was quantified by real-time PCR and proteins were detected by immunohistochemistry and Western blotting.

Treatment of cells with 1 mM NaB or 1 nM TGF $\beta$ 1 for 4 d decreased cell proliferation with a concomitant increase in the cell cycle protein p21. Real-time PCR analysis showed a significant increase in 7B2 mRNA after NaB and TGF $\beta$ 1 treatment. PC2 mRNA was down regulated by NaB while PC1 mRNA was unchanged. TGF $\beta$ 1 stimulated PC1, but not PC2 mRNA levels. Changes in PC1 and PC2 protein were similar to changes in the mRNAs, but the differences were not significant.

These results indicated that NaB and TGF $\beta$ 1 inhibit pituitary cell proliferation and regulate the expression of 7B2, PC1, and PC2 in a cell culture model of pituitary tumors. Our results also indicate that inhibition of pituitary cell proliferation is associated with increased expression of 7B2 mRNA.

**Key Words:** 7B2; prohormone convertase; PC1/3; PC2; TGF $\beta$ 1; sodium butyrate; HP75; real-time PCR; Light-Cycler; SYBR green I.

## Introduction

Proprotein convertases are a family of subtilisin-like proteases that produce mature functional proteins of peptides by cleaving their precursors at usually pairs of basic residues (1). Proprotein convertase 1/3 (PC1) and PC2 are largely expressed by neuroendocrine cells and tumors, where they are involved in the processing of prohormones and proneuropeptides (2). 7B2 is an acidic protein present in the secretory granules of neuroendocrine cells and functions as a specific chaperone for PC2. The biological importance of 7B2 and PC2 in pituitary tumor development is illustrated by the observation that 7B2-null mice lack PC2 activity, and develop pituitary adrenocorticotrophic hormone (ACTH) hypersecretion (4). Although the functional link between PC2 and 7B2 implies that expression of these genes are coordinately regulated, there are very few studies that have concomitantly analyzed the regulation of both genes in vitro (3). In situ hybridization studies on rat brain have shown that while all cells containing PC2 transcripts also contained 7B2 transcripts, there were cells containing 7B2 without PC2, suggesting other roles for 7B2 (5).

Recent studies have shown that ACTH secretion is negatively modulated by the intracellular level of 7B2 in ACTH-producing AtT20 cells (6). A recent study showed that ACTH hypersecretion in 7B2 null mice is mediated in part through regulation of dopaminergic pathway as the pituitary of 7B2 null mice contained only a quarter of the normal levels of dopamine and circulating ACTH in the null mice was lowered by bromocriptine treatment (7). PC1, PC2, and 7B2 are expressed by human pituitary adenomas (8,9), but their roles in hormone processing and secretion in human pituitary tumors are unknown and the regulation on 7B2, PC1, and PC2 in human pituitary adenomas has not been previously examined.

Received July 31, 2003; Revised September 10, 2003; Accepted October 7, 2003.

Author to whom all correspondence and reprint requests should be addressed: R. V. Lloyd, MD, Mayo Clinic, Department of Laboratory Medicine, and Pathology, 200 First Street, SW, Rochester, MN 55901. E-mail: lloyd.ricardo@Mayo.ed

Histones are part of the core proteins of nucleosomes. Acetylation and deacetylation of these proteins play a role in the regulation of gene expression. Acetylation generates a more open DNA conformation, with increased access to the DNA by transcription factors (10). The degree of acetylation is controlled by the opposing activities of histone acetyltransferases (HATs) and histone deacetylases (HDACs). It has been shown that cyclic adenosine monophosphate response element-binding proteins (CBP/p300), which act as coactivators for a numbers of transcription factor complexes, are members of a group of proteins with intrinsic HAT activity (11). HDACs, in addition to deacetylation of histone, may also regulate gene expression by deacetylation of transcription factors, such as p53, GATA-1, TFIIE, TFIIF (12).

Histone deacetylase inhibitors (HDACI), which inhibit HDAC activity, have been shown to be potent inducers of cell growth arrest, differentiation, and/or apoptotic cell death of transformed cells in vitro and in vivo (10). The action of HDACI on gene expression is selective. For example, the expression of approx 2% of cellular genes changes in response to treatment with TSA, a specific HDAC inhibitor (13). Butyrates represent short-chain fatty acids that are one of the structural classes of the HDACI, and one of its analogs is approved currently for use in clinical trials (14). The molecular basis of NaB-induced growth impairment are mainly ascribed to increased p21<sup>WAF1/Cip1</sup> and p27<sup>kip1</sup> proteins, in which p21mRNA is up-regulated, while p27 protein degradation is down-regulated (15,16). As 7B2, PC1, and PC2 promoter regions also contain cyclin adenosine response elements (CRE), these genes are expected to be up-regulated with NaB treatment (3,17,18).

The HP75 cell line, which was derived from a human non-functioning gonadotrophic adenoma, was established using SV-40 large T antigen in our laboratory (19). The cell line has been shown to express PC1, PC2, and 7B2 along with small amounts of FSH, LH, and CgA. This is one of the few available human pituitary cell lines, so it is an invaluable model to examine the biology and pathophysiology of 7B2, PC1, and PC2 regulation in humans. We and others have shown that this cell line is responsive to TGFβ1 superfamily members, TGFβ1 (19), and activin after transfection of wild-type activin receptor (20). Various studies from our laboratory (19,21,22) and by others (20,23) have shown that TGFβ1 and other members of this superfamily play critical roles in growth regulation and secretion of anterior pituitary hormones. In this study, we analyzed cell proliferation, and expression of 7B2, PC1, and PC2 mRNA and their proteins to study regulation of these genes in HP75 cells. Our result showed that NaB and TGFβ1 down-regulated HP75 cell proliferation with increased p21 expression. NaB up-regulated 7B2 mRNA expression and down-regulated PC2 mRNA, while TGFβ1 up-regulated 7B2 mRNA and up-regulated PC1mRNA, but not PC2 mRNA. The results indicate that both NaB and TGFβ1 have important roles in 7B2

mRNA expression but they have different regulatory effects on neuroendocrine-specific proconvertase expression.

## Results

### Cell Proliferation

Treatment with 1 nM TGFβ1 and 1 mM NaB on HP75 decreased cell proliferation compared to the control group (TGFβ1, 76.8 ± 7.3%; NaB, 49.7 ± 8.2%) (Fig. 1A). TGFβ1 and NaB treatment led to a decrease in thymidine incorporation (TGFβ1, 89.8 ± 14.4%; NaB, 56.8 ± 12.7%) (Fig. 1B). NaB was more effective than TGFβ1 in inhibiting cell growth. Analysis of cell proliferation by proliferating cell nuclear antigen (PCNA) showed a significant decrease in the NaB-treated group (Fig. 1C).

Treatment with TGFβ1 and NaB led to a significant increase in p21 (Fig. 2A). Although the number of p27 positive cells increased after NaB and TGFβ1 treatment, these difference were not significant (Fig. 2B). Western blot analysis for p21 and p27 supported the immunohistochemical findings (Figs. 2C–E).

### Expression Levels of 7B2, PC1, and PC2

Expression of 7B2, PC1, and PC2 mRNA in HP75 cells was analyzed by LightCycler (Roche). An amplification plot of fluorescence versus cycle number for the standards between 10<sup>3</sup> and 10<sup>6</sup> copies/capillary and targets were performed. A signal was not present in the no-template control. A standard curve was then constructed by plotting the cycle number of crossing points versus the standard log concentration. A melting curve analysis, which was the first negative derivative of fluorescence versus temperature, was done. Only one melting peak for each sample (standards and targets) was observed. There was no signal in the no-template sample. The final results of real-time PCR analysis are shown in Figs. 3A–C. The expression of the housekeeping gene hHPRT was used to normalize for mRNA variation between different samples. hHPRT expression, which was used as an internal control, correlated well with another housekeeping gene (GAPDH) (data not shown). NaB treatment increased 7B2 mRNA expression in HP75 cells more than 2.9-fold above control levels, while TGFβ1 treatment increased 7B2 mRNA 1.4-fold. In the presence of TGFβ1, PC1 mRNA expression increased approx 2.5-fold while NaB treatment did not change PC1 mRNA. PC2 mRNA expression was significantly decreased by NaB treatment. Negative controls including omission of reverse transcriptase or use of no-template samples did not give a positive signal. Gel analysis showed a specific band with the expected sizes for 7B2 and PC1. The real-time PCR efficiency was calculated from the slopes in the LightCycler Software 3.5 (Roche Diagnostics). The corresponding real-time PCR efficiency of one cycle in the exponential phase was calculated according to the equation:  $E = 10[-1/\text{slope}]$ . The efficiency of 7B2, PC1, and PC2 were 1.95, 1.89, and

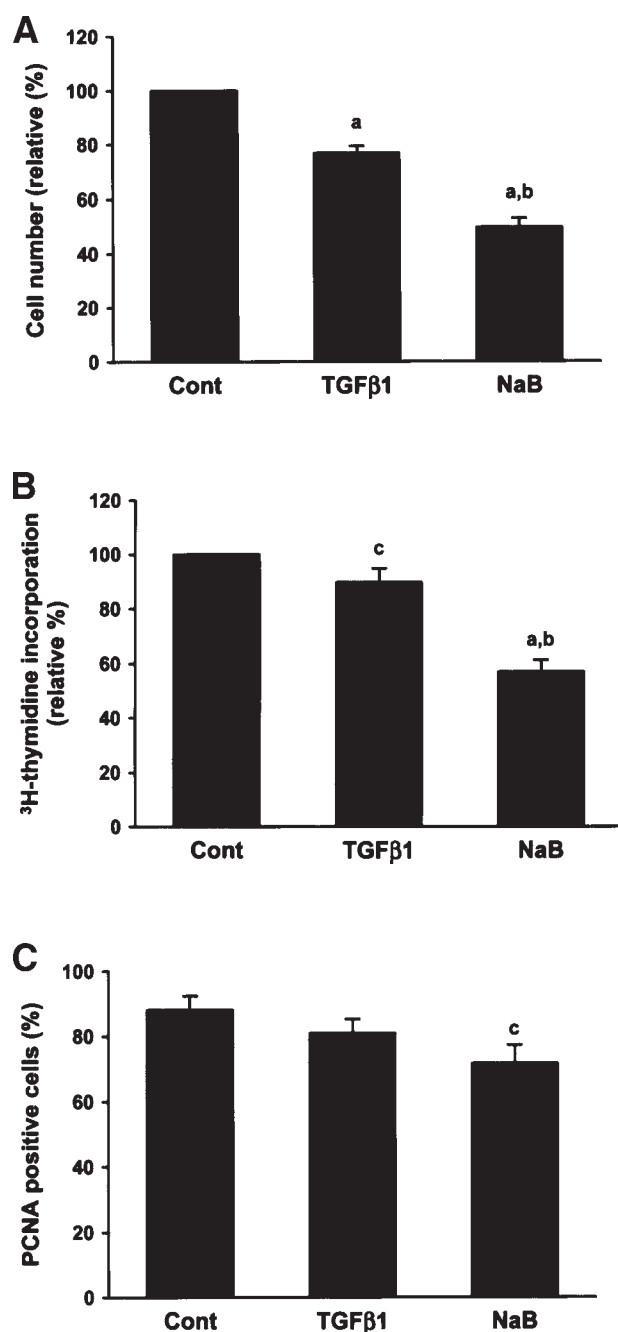


**Fig. 1.** Effect of TGFβ1 or NaB treatment on HP75 cell proliferation. (A) Cell numbers per dish after 4-d treatment. (B) <sup>3</sup>H-thymidine incorporations. Data are from nine experiments with duplicate dishes. Results are expressed as percentage change compared with control groups and are shown as mean ± SEM. **a:** Compared to control group ( $p < 0.01$ ); **b:** compared to TGFβ1 group ( $p < 0.01$ ); **c:** compared to control group ( $p < 0.05$ ). Cont: control group, TGFβ1: 1 nM TGFβ1 treatment group; NaB: 1 mM sodium butyrate treatment group. (C) Immunocytochemical analysis of PCNA.

1.83, respectively. Sequence analysis of ligated PCR products for 7B2, PC1, and PC2 were performed to confirm the primer designs. The result agreed with the sequence from the GeneBank database.

Western blot analysis of PC1 and PC2 with densitometric analysis showed a slight increase in PC1 after TGFβ1 treatment, but no change in PC1 after NaB treatment (Fig. 4A). PC2 protein was decreased after NaB treatment, but TGFβ1 treatment had no effect on PC2 (Fig. 4B). 7B2 were not detected by Western blotting in the HP75 cells, although positive-control pituitary tissues expressed 7B2 (data not shown).

## Discussion

Using the HP75 human pituitary adenoma cell line as a model, we showed that NaB and TGFβ1 treatment decreased proliferation of these tumor cells in vitro. The inhibition of cell proliferation was more marked with NaB treatment than with TGFβ1. Inhibition of cell growth was accompanied by significant up-regulation of p21<sup>WAF1/Cip1</sup>. 7B2 gene expression was also influenced by TGFβ1 and NaB treatment. NaB up-regulated expression of 7B2 mRNA and down-regulate PC2 mRNA, and TGFβ1 up-regulated 7B2 mRNA and PC1 mRNA.

7B2 has been shown to be a molecular chaperone preventing premature activation of proPC2 as these proteins move to the Golgi complex and secretory granules (24). *In situ* hybridization studies on rat brain have shown that while all cells containing PC2 transcripts also contained 7B2 transcripts, there were cells containing 7B2 without PC2, suggesting other roles for 7B2 (5). 7B2-null mice not only lack PC2 activity, but they also develop adrenocorticotrophic hormone (ACTH) hypersecretion, suggesting that 7B2 may regulate hormone secretion (4).

Our study showed up-regulation of 7B2 mRNA expression by NaB and TGFβ1 in HP75 cells. The 21 kDa 7B2 protein was not detected in HP75 cells while it was easily detectable in a primary pituitary null cell adenoma used as a positive control. Marcinkiewicz et al. demonstrated that normal pituitary cells expressed 7B2mRNA but the 7B2 protein in corticotrophs, somatotrophs, and lactotrophs could not be visualized by immunocytochemistry, and they postulated that the discrepancy was due to the storage capacity and/or turnover (balance between biosynthesis and degradation) (25). As HP75 cells have been shown to have few secretory granules (19), the storage capacity for 7B2 is most likely decreased. However, impairment of translation and/or degradation could also be a potential reason for the discrepancy between 7B2 mRNA and protein expression in HP75 cells.

The autocatalytic conversion of proPC1 occurs in the endoplasmic reticulum and its activation takes place in the trans Golgi network (TGN) and immature granules (26). Various studies suggest that proPC2 conversion to mature PC2 may be initiated in the TGN, but takes place mainly in the secretory granules (2). Our ultrastructural studies of HP75 showed only a few secretory granules (19), so the processing of PC2 as well as 7B2 in these cells may be different from other neuroendocrine cells with more secretory granules.

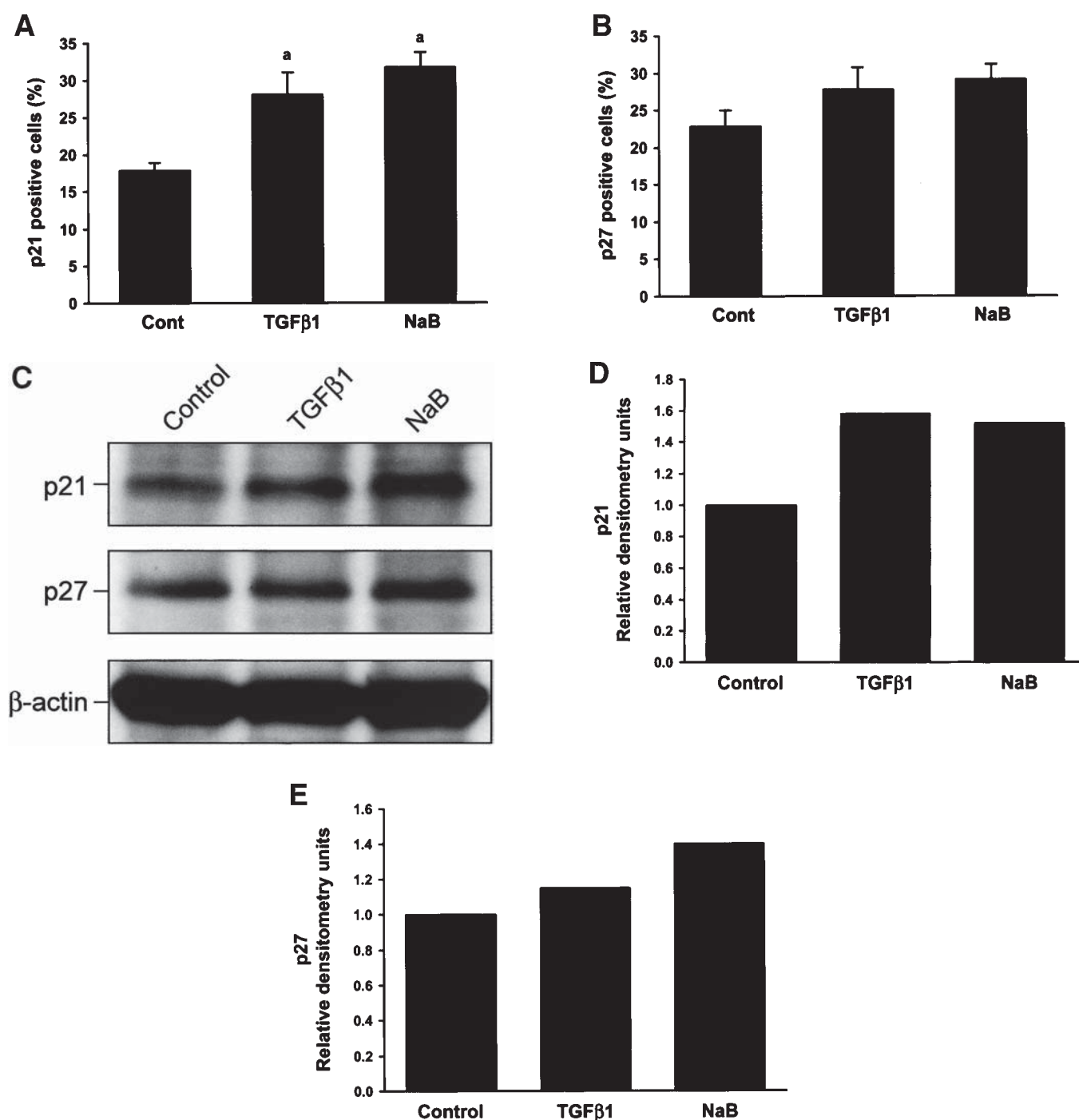


**Fig. 2.** Immunocytochemical analysis of p21 and p27 in HP75 cells after treatment with TGFβ1 or NaB. The percentage of positive cells are expressed as mean cell count  $\pm$  SEM from nine experiments. (A) Immunostaining for p21.  $p < 0.001$  compared to control. (B) Immunostaining for p27. (C) Western blotting for p21, p27, and  $\beta$  actin. Fifty micrograms of protein were used per lane as described in Materials and Methods. Western blots from three separate experiments were analyzed by densitometry. Results of one representative Western blot experiment is shown. Densitometric analysis of the fold-change for p21 (D) and p27 (E) are shown.

Our results demonstrated increased p21 after NaB treatment in the HP75 cell line. NaB acts as HDACI and leads to cell growth impairment and cell differentiation. Part of the molecular bases of NaB-induced growth impairment is ascribed to increased p21. The cyclic adenosine monophosphate response element-binding protein (CBP) has intrinsic

HAT activity and the promoter regions of 7B2 and PC2 contain CRE binding sites. Our study revealed a decrease in both PC2 mRNA and protein in HP75 cells after NaB treatment for 4 d, with up-regulation of 7B2 mRNA. Petit-Turcotte and Paquin observed that treatment with NaB for 24 h up-regulated 7B2 protein level and PC2 protein and



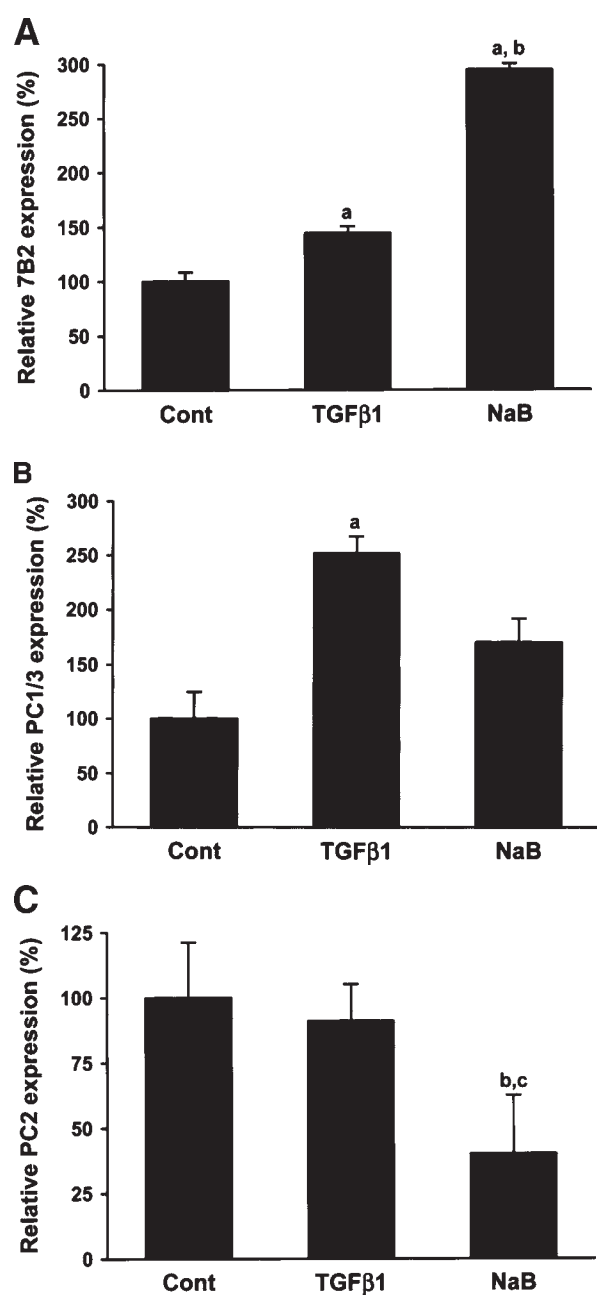


**Fig. 3.** Effect of treatment with TGFβ1 or NaB on 7B2, PC1, and PC2 mRNA expression in HP75 cells. Data were from nine experiments with duplicate real-time PCR measurements. Results were normalized with the expression of hHPRT housekeeping gene, expressed as percentage change compared with control groups and shown as mean ± SEM. (A) 7B2 mRNA expression. (B) PC1/3 mRNA expression. (C) PC2 mRNA expression. a: compared to control group ( $p < 0.01$ ); b: compared to TGFβ1 group ( $p < 0.01$ ); c: compared to control group ( $p < 0.05$ ).

coordinated regulation of both proteins by modulators of protein kinase A and C in mouse P19 embryonal carcinoma with neuronal differentiation (27). Differences in their experiments and ours on PC2 expression could be related to different cell lines, the duration of treatment, and/or concentration of NaB used. A coordinated increase in the intracellular

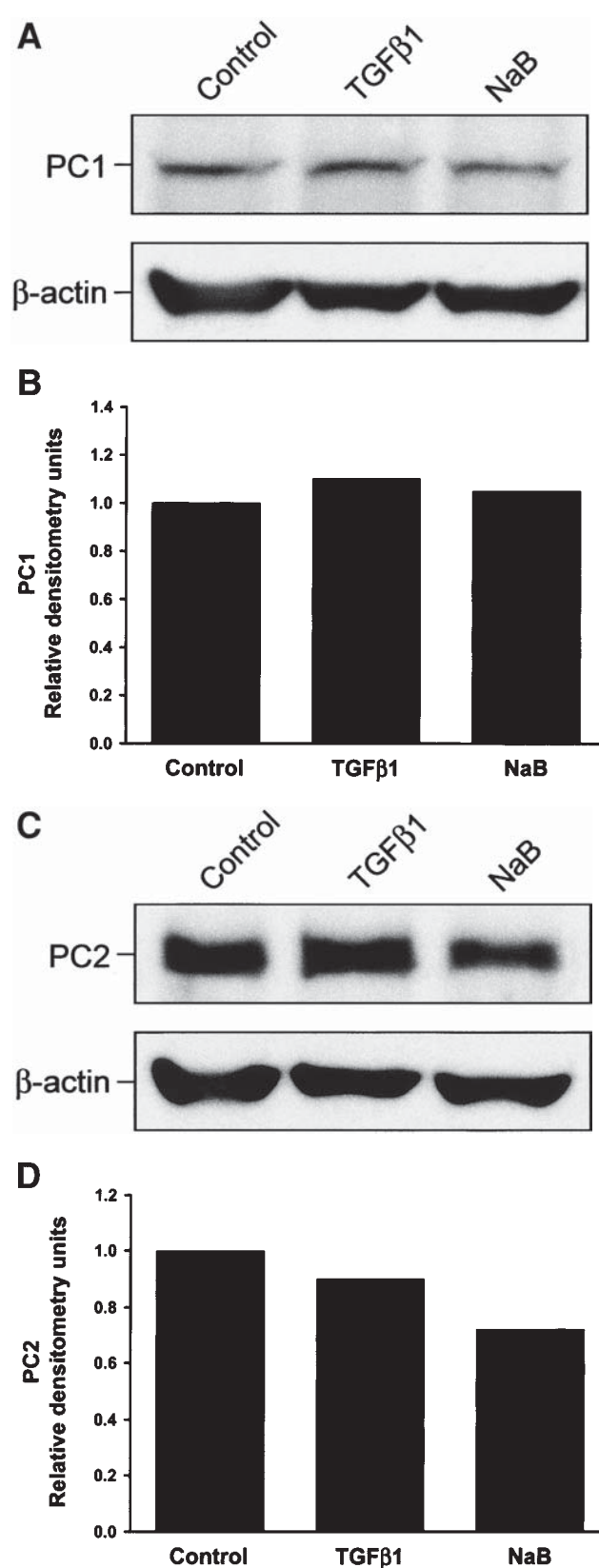


**Fig. 4.** Western blotting for (A) PC1/3 (PCI) with densitometric analysis of fold-change for PC1 (B), and for PC2 (C) with densitometric analysis of fold-change for PC2 (D) are shown. Fifty micrograms of protein was used per lane as described in Materials and Methods. Western blots from three separate experiments were analyzed. Results of one representative experiment are shown.

levels of immunoreactive 7B2 and PC2 has been observed in rMTC 6-23 cells treated with dexamethasone for 1–2 d (28).

The mechanism of gene expression with HDACi is due to relaxation of DNA because of histone hyperacetylation and this mechanism influences many genes. In contrast, signaling from TGF $\beta$ 1 is transmitted to target genes via its specific receptors, TGF $\beta$ 1 receptor I and II, and Smad proteins (29). The HP75 cell line has been shown to decrease cell proliferation in the presence of TGF $\beta$ 1 or in overexpression of wild-type activin type IB receptor Alk4, which suggests that the intracellular signaling pathway for TGF $\beta$ 1 superfamily is functional in HP75 cells (20). In this study, TGF $\beta$ 1 treatment increased p21 mRNA expression, suggesting that the signaling pathway to p21 gene (i.e., via T $\beta$ RE) (30) is also conserved. TGF $\beta$ 1 up-regulated 7B2 mRNA but did not influence PC2mRNA in HP75 cells. Both 7B2 and PC2 protein levels increased after treatment with PMA and dibutyryl-cAMP in mouse P19 embryonal carcinoma with neuronal differentiation (27). The results of our studies with TGF $\beta$ 1 suggest that 7B2 and PC2 expression may be differentially sensitive to regulatory agents and may reflect other roles of 7B2 in addition to that of a chaperone for PC2 in HP75 cells.

Real-time PCR using SYBR green I dye-based detection was a rapid and sensitive method to quantify gene expression with high reproducibility (31). Competitive RT-PCR is a PCR endpoint analysis that permits only semiquantitative analysis at a low level of sensitivity and requires multiple assays. Densitometric analysis of conventional PCR must be performed in the linear phase of amplification rather than the plateau phase. In order to validate the results of real-time PCR, we performed gel analysis and melting-curve analyses. We also showed that the results of the real-time PCR for PC1 and PC2 mRNA with TGF $\beta$ 1-treated group were in accordance with our previous studies using densitometric analysis with conventional PCR (8).

In summary, our results showed that NaB and TGF $\beta$ 1 decreased cell proliferation with increase p21 expression in HP75 cells. NaB also increased 7B2 mRNA expression and down-regulated PC2 mRNA, while TGF $\beta$ 1 up-regulated 7B2 and PC1mRNAs, but not PC2 mRNA. These results suggest that 7B2 mRNA expression is regulated by different pathways in pituitary cells and that inhibition of cell proliferation is associated with increased expression of 7B2 mRNA in HP75 cells.

## Materials and Methods

### Cell Culture

An immortalized cell line derived from a human nonfunctioning pituitary adenoma, HP75 cell, was grown in complete Dulbecco's modified Eagle's medium (DMEM) with 15% horse serum and 2.5% fetal bovine serum with 1  $\mu$ g/mL insulin and 1% antibiotics (all from Invitrogen, Carlsbad, CA). The HP75 cells were plated onto 35 mm plastic dishes

at approx  $0.1 \times 10^6$  cells/dish for thymidine incorporation test or 25 cm<sup>2</sup> cell culture flask at  $0.5 \times 10^6$  cells/flask for other tests. The cells were treated with final concentration of  $10^{-9}$  M TGF $\beta$ 1 (R&D Systems, Inc., Minneapolis, MN) or  $10^{-3}$  M of sodium butyrate (Calbiochem, San Diego, CA) in complete DMEM for 4 d. The culture medium and reagents were changed every other day. A total of nine experiments were performed with the same culture condition.

### Cell Proliferation

After 4 d of treatment, the culture mediums of the dishes were changed, and 20  $\mu$ Ci 6-<sup>3</sup>H-thymidine (Perkin Elmer Life Science Products, Boston, MA) was added and incubated for 4 h. The cells were harvested and cell numbers were counted with a hemocytometer. After centrifugation, cell pellets were washed twice with PBS. The washed cells were resuspended with 1 mL of PBS. Triplicate 100  $\mu$ L aliquots of the suspension were used for liquid scintillation counting with Beckman LS6500 (Beckman Coulter, Inc., Fullerton, CA) as previously described (19).

### Immunocytochemistry

The cells were harvested and aliquots were cytocentrifuged (approx  $0.5 \times 10^6$  cells/slide) and fixed in 4% paraformaldehyde for 20 min and used for immunocytochemistry. The remained of the cells were centrifuged and used for RNA or protein extraction. Immunocytochemistry were performed with the Avidin-biotin complex peroxidase methods as previously described (32). Monoclonal antibodies to p21 (Transduction Laboratory, Lexington, KY), p27 (Transduction Laboratory), and PCNA (Dako Corporation, Carpinteria, CA) were used at 1:500, 1:1000, and 1:500 dilution, respectively. The slides were developed with diaminobenzidine chromogen. Cells were enumerated by counting a minimum of 500 cells per slide, and the results were expressed as the percentage of positive cells.

### RNA Extraction

Total RNA from the cultured cells were extracted using TRIzol reagent (Invitrogen) and used for analysis of 7B2, PC1, PC2, and hHPRT mRNA expression by real-time PCR. The concentration of the total RNA solutions were measured with a spectrophotometer and aliquoted samples were stored at  $-70^\circ\text{C}$  until use.

### Reverse Transcription Reaction

First-strand cDNA was prepared from the total RNA by using a ProSTAR<sup>TM</sup> first-strand RT-PCR kit (Stratagene, LaJolla, CA) following the manufacturer's instruction. The reverse transcription reaction was carried out in a total volume 50  $\mu$ L with 5  $\mu$ g of total RNA, containing 300 ng of oligo (dT) primer, 1X RT buffer, 50 U of StrataScript<sup>TM</sup> reverse transcriptase, 40 U of RNase block ribonuclease inhibitor, and 4 mM dNTPs. In terms of the order of adding reaction components, total RNA and oligo-dT were mixed first, heated

**Table 1**  
Primers and Cycling Conditions for the LightCycler Real-Time PCR

Gene	Primer sequence <sup>a</sup> (5' - 3')	Site	Length of product (bp)	Annealing temperature (°C)/time (s)	Extensin temperature (°C)/time (s)	Acquisition temperature (°C)/time (s) or place	Cycle numbers	Range of the standards (copies/capillary)
7B2	P1 CATTGGGGTCCTTTTGGCAAC	Exon 3	287	68/2	72/12	72/at the end of extension	35	10 <sup>3</sup> –10 <sup>6</sup>
	P2 CGCTTTCGTCTCTCTCTCCC	Exon 5						
PC1	P1 TGGGCTGAACAACAGTATGAA	Exon 3	248	64/5	72/10	72/at the end of extension	40	10 <sup>2</sup> –10 <sup>5</sup>
	P2 TTGGCATAAATGTCCGTGTGA	Exon 4						
PC2	P1 CCTGGCCTCCAATAATG	Exon 5,6	273	64/5	72/11	83/3 <sup>c</sup>	45	10 <sup>1</sup> –10 <sup>4</sup>
	P2 GCGCTGTAGATGTCAATCA	Exon 8						
HPRT <sup>b</sup>			181	55/15	72/15	55/at the end of annealing	45	From 10 <sup>2</sup> to 10 <sup>5</sup> copies RNA

<sup>a</sup>P1: upper primer; P2: lower primer.

<sup>b</sup>From LightCycler-h-HPRT Housekeeping Gene Set.

<sup>c</sup>As some sample amplicons had primer–dimers with melting temperature lower than 83°C on PC2 analysis, a high-temperature acquisition segment was added in order to avoid influence of the dimers. s=seconds.

to 65°C for 5 min, and cooled at room temperature for 10 min to allow the primers to anneal to the RNA until addition of the remaining reaction components. The mixtures were allowed to proceed for 60 min at 42°C, followed by 5 min of heating at 95°C and rapid cooling on ice. The cDNA solutions were aliquoted and stored at –70°C until use.

Primers were designed using Oligo primer analysis software version 5.0 (Molecular Biology Insights, Cascade, CO). All primers were designed to cross intronic sequences. The sequences of primers are shown in Table 1.

#### PCR Standard Synthesis

External DNA standards for 7B2, PC1, and PC2 were constructed by TA-cloning of PCR fragments into pGEM-T easy vector (Promega, Madison, WI) according to standard protocols. cDNA from a human gonadotroph adenoma was used as template. The PCR fragments were generated by conventional RT-PCR with the same primers as described above. Ligated fragments were transformed into XL1-blue competent cells (Stratagene), and a single colony was recovered and cultured. The plasmid DNA was prepared by using the Qiagen mini-prep (Qiagen, Valencia, CA) according to the protocol. The sequence identity of the cloned fragment in the purified plasmid DNA constructs was verified by DNA sequencing using M13 forward primer at Mayo Molecular Core Facility. After confirmation of the sequence, the plasmid with the fragment was transformed into the XL-1 blue competent cells, cultured as a single colony, and purified using Qiagen midi-prep (Qiagen). The plasmid DNA were digested by *EcoRI* and the fragments were purified by 1% gel electrophoresis followed by excision of the band of the correct molecular weight and extracted with an Ultrafree-DA centrifugal filter device (Millipore, Bedford, MA) and concentrated using Microcon YM-100 centrifugal filter (Millipore). In order to prevent contamination of bromophenol blue (BPB), a loading buffer containing xylene cyanol (CX) was used. Concentration of *EcoRI* fragments were

determined by measuring the OD at 260 nm using a spectrophotometer. Copy numbers were calculated according to the following equation: Copy number (copies/μL) =  $(6.023 \times 10^{23} \text{ molecules/mole} \times \text{OD}_{260} \times 50 \text{ μg/mL/OD} \times 10^{-9} \text{ g/μL}) / (662 \text{ molecular weight/bp} \times \text{EcoRI fragments bp})$ . The standard solutions were adjusted to a concentration of  $0.5 \times 10^7$  copies/μL, aliquoted, and stored at –70°C. Just before the PCR reaction, the standard solution was diluted 1:10 with nano-pure water and used making standard curve.

#### Real-Time PCR

PCR amplification and analysis were performed with a LightCycler instrument (Roche Diagnostics, Alameda, CA) and the software version 3.0, respectively, by using SYBR Green I as a double-strand DNA specific binding dye. Amplification was carried out in a total volume of 20 μL containing 0.5 μM of each primer, 4 mM MgCl<sub>2</sub>, 2 μL LightCycler FastStart DNA master SYBR green I, and 2 μL of sample or standard cDNA prepared as described above. The standards and the samples were simultaneously amplified using the same reaction master mixture. For each primer combination optimal MgCl<sub>2</sub> concentration and annealing temperature were experimentally determined. For all primers 4 mM MgCl<sub>2</sub> was optimal. The reactions were incubated at 95°C for 10 min to activate the polymerase followed by amplification cycles. PCR cycle conditions for each gene were shown in Table 1. Fluorescence was acquired at 72°C for 7B2 and PC1, at 83°C for PC2 because of persistent primer–dimers when the melting temperature was lower than 80°C (33). After cycling, melting curves of the PCR products were performed by stepwise increase of the temperature from 69°C to 95°C with a temperature transition rate of 0.1°C/s.

hHPRT mRNA expressions were measured using LightCycler–h-HPRT Housekeeping Gene Set and LightCycler–FastStart DNA Master Hybridization Probes (Roche diagnostics) according to the manufacturer's protocol. Reverse

transcription reaction was carried out in a total volume 25  $\mu$ L with 6.25  $\mu$ L of each RNA template ( $10^6$  to  $10^2$  copies/ $\mu$ L) that were provided from the hHPRT housekeeping gene set. The other RT-reaction conditions were the same as described above. Polymerase chain reactions for hHPRT were performed according to the manufacturer's protocol. The final result are expressed as fold of induction according to the following equation: Relative expression of the target gene = (Copies of target gene)/(Copies of hHPRT). Values for controls were finally set to 100%.

To ensure that the correct product was amplified, all amplicons were separated by 2% agarose gel electrophoresis and stained with 0.75  $\mu$ g/mL of ethidium bromide. Gel analysis was performed with Gel Doc system and Quantity One Software ver. 4.3.0 (Bio-Rad Laboratories, Hercules, CA). To check for contamination, all PCR amplifications were performed with water. An RT-negative sample was also used as a negative control.

### Western Blotting

Total protein was extracted with a lysis buffer (Immunoprecipitation Kit, Roche) and quantified with DC Protein Assay Kit (Bio-RAD). One-dimensional sodium dodecyl sulfate polyacrylamide gel electrophoresis (SDS-PAGE) was performed with a 12% or 8.5% gel as previously reported (34). The electrophoresed proteins (50  $\mu$ g) were transferred to a PVDF membrane and subjected to immunoblot analysis with monoclonal antibodies to p21 (1/500 dilution), and p27 (1/500) and polyclonal antisera to 7B2 (1/1000, Phoenix, Pharmaceuticals, Inc., Belmont, CA), PC1 (1/1000) and PC2 (1/2000, gift from Dr. D. Steiner). The reactions were detected with ECL Western blotting detection reagents and analysis system (Amersham Biosciences Corporation, Piscataway, NJ). In order to correct for protein loading,  $\beta$ -actin monoclonal antibody (1/1500, Sigma) was used. Quantification of the bands by densitometry was carried out with Chemi Doc system and Quantity One Software (Bio-Rad laboratories). Western blotting was performed on three independent experiments and the result was shown as the mean.

### Statistical Analysis

A total of nine experiments for immunocytochemistry and RT-PCR was performed. Results were expressed as the mean  $\pm$  SEM. For statistical evaluations data were analyzed by t-test. Differences were considered significant at  $p < 0.05$ .

### Acknowledgments

We thank Dr. Donald Steiner, University of Chicago, for PC1/3 and PC2 antisera. The encouragement of Prof. Kiyotaka Fujii, MD, Department of Neurosurgery, Kitasato University School of medicine and Takeo Ishidate, MD, Director of The Kitasato Institute Medical Center Hospital in the performance of these studies is greatly appreciated. Supported in part by NIH CA90249.

### References

- Seidah, N. G. and Chretien, M. (1999). *Brain Res.* **848**, 45–62.
- Mullar, L. and Lindberg, I. (1999). *Prog. Nucleic Acid Res. Mol. Biol.* **63**, 69–108.
- Mbikay, M., Seidah, N. G., and Chretien, M. (2001). *Biochem. J.* **357**, 329–342.
- Westphal, C. H., Muller, L., Zhou, A., et al. (1999). *Cell* **96**, 689–700.
- Seidel, B., Dong, W., Savaria, D., Zheng, M., Pintar, J. E., and Day, R. (1998). *DNA Cell Biol.* **17**, 1017–1029.
- Bergeron, F., Sirois, F., and Mbikay, M. (2002). *FEBS Lett.* **512**, 259–262.
- Laurent, V., Kimble, A., Peng, B., et al. (2002). *Proc. Natl. Acad. Sci. USA* **99**, 3087–3092.
- Jin, L., Kulig, E., Qian, X., et al. (1999). *Pituitary* **1**, 187–196.
- Jin, L., Zhang, S., Bayliss, J., et al. (2003). *Endocr. Pathol.* **14**, 37–48.
- Marks, P. A., Richon, V. M., and Rifkind, R. A. (2000). *J. Natl. Cancer Inst.* **92**, 1210–1216.
- Ogryzko, V. V., Schiltz, R. L., Russanova, V., Howard, B. H., and Nakatani, Y. (1996). *Cell* **87**, 953–959.
- Gu, W. and Roeder, R. G. (1997). *Cell* **90**, 595–606.
- Van Lint, C., Emiliani, S., and Verdin, E. (1996). *Gene Expr.* **5**, 245–253.
- Warrell, R. P. Jr., He, L. Z., Richon, V., Calleja, E., and Pandolfi, P. P. (1998). *J. Natl. Cancer Inst.* **90**, 1621–1625.
- Archer, S. Y., Meng, S., Shei, A., and Hodin, R. A. (1998). *Proc. Natl. Acad. Sci. USA* **95**, 6791–6796.
- Moretti, A., Borriello, A., Monno, F., et al. (2002). *Eur. J. Cancer* **38**, 2290–2299.
- Ohagi, S., LaMendola, J., LeBeau, M. M., et al. (1992). *Proc. Natl. Acad. Sci. USA* **89**, 4977–4981.
- Jansen, E., Ayoubi, T. A., Meulemans, S. M., and Van de Ven, W. J. (1995). *J. Biol. Chem.* **270**, 15391–15397.
- Jin, L., Kulig, E., Qian, X., Scheithauer, B. W., Eberhard, N. L., and Lloyd, R. V. (1998). *Endocr. Pathol.* **9**, 169–184.
- Danila, D. C., Zhang, X., Zhou, Y., Haidar, J. N. S., and Klibanski, A. (2002). *J. Clin. Endocrinol. Metab.* **87**, 4741–4746.
- Qian, X., Jin, L., Grande, J. P., and Lloyd, R. V. (1996). *Endocrinology* **137**, 3051–3060.
- Jin, L., Qian, X., Kulig, E., et al. (1997). *Am. J. Pathol.* **151**, 509–519.
- Hentges, S. and Sarkar, D. K. (2001). *Front. Neuroendocrinol.* **22**, 340–363.
- Braks, J. A. and Martens, G. J. (1994). *Cell* **78**, 263–273.
- Marcinkiewicz, M., Touraine, P., Mbikay, M., and Chretien, M. (1993). *Neuroendocrinology* **58**, 86–93.
- Shennan, K. I., Taylor, N. A., Jermany, J. L., Matthews, G., and Docherty, K. (1995). *J. Biol. Chem.* **270**, 1402–1407.
- Petit-Turcotte, C. and Paquin, J. (2000). *Peptides* **21**, 365–372.
- Barbero, P. and Kitabgi, P. (1999). *Biochem. Biophys. Res. Commun.* **257**, 473–479.
- de Caestecker, M. P., Piek, E., and Roberts, A. B. (2000). *J. Natl. Cancer Inst.* **92**, 1388–1402.
- Datto, M. B., Yu, Y., and Wang, X. F. (1995). *J. Biol. Chem.* **270**, 28623–28628.
- Castello, R., Estelles, A., Vazquez, C., et al. (2002). *Clin. Chem.* **48**, 1288–1295.
- Lloyd, R. V., Jin, L., Qian, X., and Kulig, E. (1997). *Am. J. Pathol.* **150**, 401–407.
- Pfaffl, M. (2001). In: *Rapid cycle real-time PCR, methods and applications*. Meuer, S., Wittwer, C., and Nakagawara, K. (eds.). Springer: Heidelberg.
- Lloyd, R. V., Jin, L., Qian, X., Scheithauer, B. W., Young, W. F. Jr., and Davis, D. H. (1995). *Am. J. Pathol.* **146**, 1188–1198.